

## A SYSTEM FOR RECORDING PHASE PATH VARIATIONS OF IONOSPHERIC REFLECTIONS

J. Hanumath Sastri, K.B. Ramesh  
and  
K.S. Ramanamorthy

### Abstract

An experimental set-up developed for continuous recording of the phase path variations of reflections at normal incidence from discrete regions of the terrestrial ionosphere is described. Salient features of the system design and hardware implementation of the same are presented. The phase path sounder, which is currently operated on a probing frequency of 5.0 MHz at the Kodalkanal Observatory, comprises of a broadband transmitter, phase coherent receiver(s), frequency synthesizer, timing and logic circuits and analog recording facilities. Typical features of the phase path variations of reflections from ionospheric F-region over Kodalkanal derived from recent data runs are discussed and the resourcefulness of the system for diagnostic studies of the equatorial ionosphere is outlined.

**Key words:** ionosphere - phase path - travelling ionospheric disturbances (TIDs)

### 1. Introduction

Structures or irregularities of distinct categories are well known to exist in the plasma density in the earth's ionosphere. A variety of radio techniques have been used over the past three decades to study the characteristics and horizontal movements of the wavelike irregularities in the plasma density known as 'travelling ionospheric disturbances' (TIDs). It is generally accepted that TIDs correspond to disturbances in the neutral gas associated with the passage of atmospheric gravity waves in the ionosphere (Yeh and Liu, 1974; Francis, 1975). Most of the published work on TIDs pertains to TID's observed at high and midlatitudes.

Although recent studies give evidence for the presence of TIDs at locations in the vicinity of the dip equator (Sterling et al. 1971; Nagpal, 1977; Sastri and Murthy, 1977; Rottger, 1977; Somayajulu, et al. 1980), there is a dearth of detailed information on such TIDs. There is thus a definite need for continued studies of TIDs at very low dip latitudes for a comprehensive understanding of their nature and source(s). Recent work showed that medium scale TIDs strongly effect ground-based observations of decametric radio emission from extraterrestrial sources (Meyer-Vernet, 1980). The effects are observed as caustic patterns in the dynamic spectra of solar decametric radio emission (Meyer-

Vernet, et al. 1981; Genova and Aubier, 1983). Detailed information on equatorial TIDs will thus be useful in modelling and assessing the terrestrial ionospheric component in the data obtained with our decameter-wave radio telescope at Gauribidanur ( $13^{\circ}36'N$ ,  $77^{\circ}26'E$ ).

Recording the changes in the phase path of pulsed radio waves reflected at vertical or near vertical incidence from the ionosphere is one of the very sensitive techniques available for the detection and study of TIDs and has been extensively used (Reddi and Rao, 1971; Srivastava et al. 1971a; Vincent, 1972; Butcher and Joyner, 1972; Schrader and Fraser, 1975). In most of the phase path sounders developed earlier (e.g. Reddi and Rao, 1967; Srivastava et al. 1971b) the phase of the ionospheric signal is compared in the receiver at intermediate frequency (IF) against that of a stable reference oscillator of a frequency differing from IF by about 20 KHz. The reference oscillator is triggered by the transmitter pulse and is thus phase coherent with it. The beat pattern across the width of the ionospheric echo is shaped and displayed on an oscilloscope for recording the movement of the beat maxima and hence phase path changes, as a fringe pattern of sloping lines on photographic film. Even though this widely used arrangement gives useful information on TIDs it suffers from some drawbacks. The major ones, in our opinion, are the requirement of an elaborate oscilloscope display system for recording and the undesirable susceptibility of the beat pattern across the width of the echo to interference effects which cause very frequent jumps or discontinuities in phase path records especially of E-region reflections. This latter lacuna renders a major chunk (more than 50 percent) of the data useless for analysis (Reddi, 1969; Schrader and Fraser, 1975). We have developed a phase

path recording system that relies on coherent detection and enables continuous recording of the phase path changes of reflections from discrete regions of the ionosphere on strip charts. The concept of coherent detection is now widely used in systems designed to measure changes in phase path and angle of arrival of pulsed HF signals reflected from the ionosphere (Balan, et al. 1979; Reddi, et al. 1980). The system is in operation since May 1983 at the Solar-Terrestrial Relationships Laboratory of the institute at Kodaikanal Observatory (dip  $3.5^{\circ}N$ ). In this paper, we present the design features of the experimental setup and hardware details of its constituent units. Preliminary results concerning the nature of the phase path variations of reflections from F-region, obtained from the first few months of recording are presented. The scope for augmenting the capabilities of the system for detailed studies of the various aspects of the equatorial ionosphere is also discussed.

## 2. The System Design

The schematic diagram of the experimental set-up is shown in Fig.1. A broadband pulse

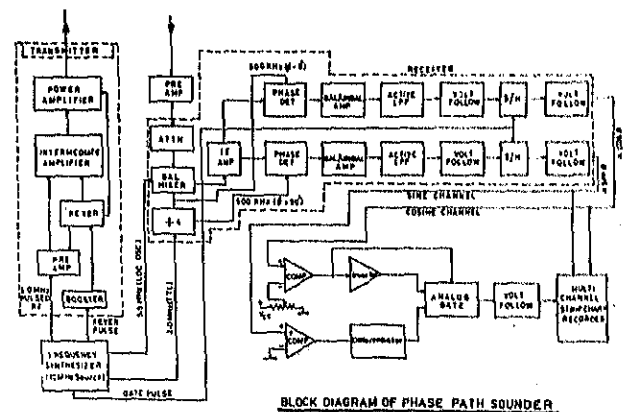


Fig. 1. Block diagram of the phase path recording system.

transmitter of C-4 type radiates  $100 \mu$  sec pulses at a repetition rate of 50 Hz with

peak power of about 2 KW. A carrier frequency ( $f$ ) of 5.0 MHz is currently being used although the system can be operated on any frequency in the range 2-20 MHz. A low level keyer pulse and a pulsed rf signal of 5V peak-to-peak generated in a frequency synthesiser unit, to be described at a later stage in this section, serve as inputs to the transmitter. The pulsed rf after reflection in the ionosphere is received by a half-wave horizontal dipole antenna, and its balanced output is coupled to the unbalanced input of the preamplifier unit of the receiver through a 1:1 balun. The receiver which is a phase coherent one, consists of a conventional mixer and an IF amplifier the IF being 500 KHz. The local oscillator frequency ( $f+500$  KHz) for the mixer is also generated in the frequency synthesiser mentioned above and is fed to the receiver. The local oscillator signal is phase coherent with the transmitter frequency. 2 MHz TTL pulses which are also generated in the frequency synthesiser unit are fed to the receiver where they are frequency divided to yield two square outputs in phase quadrature at 500 KHz. The signal IF in the receiver is then phase compared against these reference IF signals in two separate phase detectors (see block diagram of receiver in Fig.1). The outputs of the two phase detectors are separately amplified and band limited using low pass active filters. A gate pulse of 10  $\mu$  sec width occurring at a repetition rate of 50 Hz whose delay w.r.t. to the transmitter pulse can be varied is also generated in the frequency synthesiser, and is fed to the receiver to activate the sample and hold (S/H) circuits in the two quadrature channels. The filtered outputs in the quadrature channels are thus sampled and held for a period of 20 ms. From the quadrature channel outputs ( $A \cos \phi$ ,  $A \sin \phi$ ) of the receiver recorded on strip chart,

the instantaneous amplitude ( $A$ ) and the carrier phase ( $\phi$ ) and their time variations can be computed. By selecting the time delay of the gate, pulse phase path variations corresponding to specific altitude regions in the ionosphere can be recorded and studied. It is pertinent to mention here that the system does not permit the determination of the absolute values of the phase path in view of the initial  $2n\pi$  ambiguity in the measured phase angle, which is a basic limitation of the phase path technique.

The stable frequencies required for transmitter and receiver injection and for various timing circuits are all generated synchronously from a single 10 MHz crystal oscillator in the frequency synthesiser unit which thus constitutes the heart of the system. The alternative arrangement of feeding the transmitter and receiver from two independent frequency sources and maintain an acceptable level of phase coherence of the received signals requires frequency standards with an stability of better than 1 part in  $10^9$ . Such sources although available commercially are quite expensive and hence this possibility is not explored. The 10 MHz crystal oscillator used here has a long term stability better than 1 part in  $10^6$  and a short term stability an order of magnitude more and is thus quite adequate to maintain phase coherence of the signals, as the transmitter and receiver frequencies are phase locked. We have adopted the direct method of frequency synthesis where in a sequence of arithmetical operations are performed on the reference frequency to generate the various other required frequencies. This is preferred to the indirect technique of using a voltage controlled oscillator (VCO) phase locked to the reference signal because (a) it permits finer resolution and greater spectral purity in the output

and (b) it's stability is directly linked with that of the reference frequency, unlike in the indirect technique where the stability of VCO and the bandwidth of the phase lock loop (PLL) also influence the output.

The block diagram of the frequency synthesiser is shown in Fig.2. The various frequen-

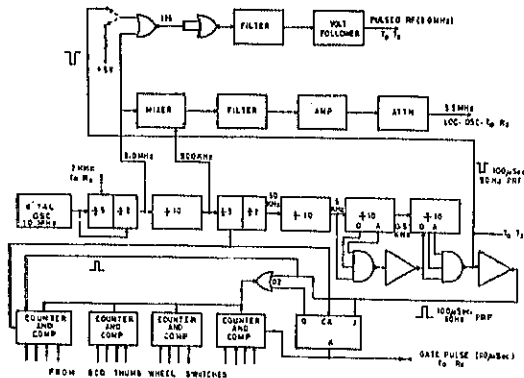


Fig. 2. Block diagram of the frequency synthesiser and selective delay pulse generator.

cies required for the individual units of the system are derived from the 10 MHz master oscillator by doing the standard operations of frequency division, mixing, filtering and adopting digital logic. The scheme is as follows. The output of the 10 MHz crystal oscillator is frequency divided to get 5 MHz, 2 MHz, 500 KHz, 500 Hz and 50 Hz. the 500 Hz and 50 Hz TTL pulses are used in conjunction with logic gates to generate the negative pulse for the transmitter Keyer unit and the positive pulse for the delay gate pulse generator. Both the pulses are of 100  $\mu$  sec duration with a repetition rate of 50 Hz and occur at the same time. The CW carrier frequency of 5.0 MHz for the transmitter is generated by filtering the 5.0 MHz square waves from the decade scaler chain. The CW 5.5 MHz L.O signal for receiver injection is derived by mixing the 5.0 MHz and 500 KHz squares and filtering the output. The filtered output is amplified and is fed to

the receiver through an attenuator. A conventional four decade counter comparator is used to generate the delay gate pulse of 10  $\mu$  sec width for activating the S/H circuits in the receiver. The 100  $\mu$  sec positive transmitter pulse and the 100 KHz pulses from the decade scaler chain serve as the initiating pulse and clock pulses respectively for the counter comparator logic.

Although strip chart recording of the quadrature outputs of the receiver permits evaluation of the phase path variations to an accuracy of about 15°, the manual scaling of the data becomes laborious and highly time consuming particularly when data are to be reduced on a routine basis. A data run typically spans about 3 hours and the chart speed used is 10 cm/min. The limitation of the manual scaling of data is thus obvious. To overcome this, a simple logic scheme has been developed in the first instance which enables strip chart recording of the phase path changes in units of  $2\pi$  radians (a wavelength of the operating frequency) for ease of scaling the data. The logic scheme, the block diagram of which is shown in Fig.1, essentially identifies the  $2n\pi$  ( $n$  is an integer, positive or negative) phase condition using both the quadrature outputs of the receiver and gives out a positive (negative) spike when the phase angle is increasing (decreasing) through  $2n\pi$ . The quadrature outputs are fed to two comparators and the comparator to which the SINE channel is fed is referenced to ground. The comparator to which the COSINE channel is fed is however referenced to a positive d.c. voltage about 70 percent of the maximum expected amplitude so much so, each time the phase angle of the received signal is close to  $2n\pi$ , the comparator A gives a positive gate pulse for the duration when the input to it exceeds

the reference level. The comparator B, on the other hand, gives a wide positive pulse of width equal to the time interval when  $A \sin \phi$  is positive ( $2m\pi < \phi < (2n+1)\pi$ ), which after differentiation yields a positive (negative) going spike when the phase angle is equal to  $2n\pi$  and  $A \sin \phi$  swings through zero from negative to positive (positive to negative). The analog gate allows the spike output of the SINE channel to pass through only when it occurs in coincidence with a gate pulse in the COSINE channel, a situation that corresponds to the phase angle around  $2n\pi$  as may be seen from the waveforms illustrated in Fig.3(a). The output recorded on a centre zero strip chart recorder will thus be a series of positive and negative spikes, the positive (negative) spike indicating a phase

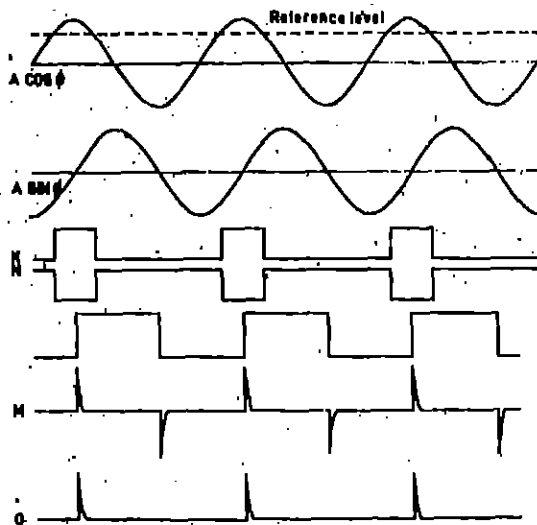


Fig. 3(a). Waveforms of the logic scheme for recording phase path changes in units of  $2\pi$  radians.

path increase (decrease) by  $2\pi$  radians. The inferred changes in phase path are practically insensitive to amplitude changes as the  $2\pi$  condition is identified from the changes in both the SINE and COSINE outputs. The logic has been extensively tested under actual operational conditions and was found to give

reliable data as may be seen from the portion of a test record reproduced in Fig.3(b).

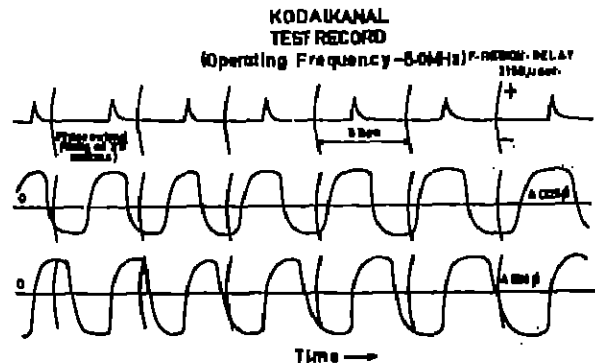


Fig. 3(b). Test record of quadrature channel outputs and phase path changes in units of  $2\pi$  radians of reflections from F-region.

The reference level for the comparator in the COSINE channel is judiciously chosen on individual occasions to minimise the errors due to fading.

### 3. The Electronics Design

#### 3.1. Transmitter (Tx)

The pulse transmitter unit rigged up is a conventional master oscillator power amplifier (MOPA) arrangement with associated power supplies. It consists of a keyer section and a rf section comprising of a three stage preamplifier, an intermediate amplifier and a final power amplifier (see Fig.1). In the keyer section, the negative TTL keyer pulse from the frequency synthesiser is boosted in a three stage amplifier employing 6SN7 and 6J5 tubes, and its positive pulse output is fed to a string of five cathode followers made up of 6L6 tubes. The outputs of the cathode followers are fed to the various amplifier stages of the transmitter i.e. the amplifiers are all keyed to the transmitter pulse and operate only for the pulse duration. The pulsed rf signal of 5V peak to peak is

amplified in a three stage preamplifier comprising of 6AG7 and 3E29 tubes. The first stage of this preamplifier is however not keyed. The amplified rf pulsed output of the preamplifier is fed to the intermediate amplifier the output of which in turn is capacitatively coupled to the final power amplifier. Eimac 4PR60B tubes are used for both the intermediate and final power amplifier stages. The final power amplifier is a push-pull configuration the balanced output of which is capacitatively coupled to the transmitting antenna through an open parallel wire feeder of  $600\Omega$  impedance. The transmitting antenna is a horizontal three element folded dipole at a height of  $\lambda/4$  from the ground. The transmitter requires unregulated d.c. voltages of +4KV, +2.5KV, +1KV and -600V and regulated voltages of +600V and +250V. The regulated power supplies used here are of commercial make. The unregulated power supplies have been rigged up in our laboratory using standard circuits adopting either electron tubes (3B24, 836) or semi-conductor diodes (ERIE XE-50) as rectifier elements. All the high voltage components (e.g. capacitors) used in the transmitter units are of indigenous origin. All the rf coils used in the Tx unit are of air core type and are wound in our laboratory.

### 3.2. Receiver (RX)

The phase coherent receiver incorporated in the experimental set-up is a general purpose commercial unit that enables measurement of the phase of the carrier signal (frequency 2-20 MHz) fed to the receiver with respect to any reference oscillator. The receiver does not contain any internal local oscillator and the selection of the operating frequency of the receiver is made by feeding in the appropriate local oscillator frequency. The unit also needs from an external source

2 MHz TTL pulses for phase detection at IF (see Fig.1). The receiver is built up of solid state electronic devices and is supplied in two sub-units: the front end preamplifier and the tail end receiver module. The preamplifier unit is housed in a weather proof box and mounted on the support pole of the receiving antenna. RG 8A/U co-axial cable is used for carrying the rf output of the preamplifier to the receiver module and also the +15V d.c. from the latter to the former. To compensate for changes in the input signal level to the receiver due to changing ionospheric conditions, a 10-position front-panel controlled attenuator is incorporated before the mixer to provide attenuation from 0 to 40 db in steps of 5 db. The IF bandwidth of the receiver is 40 KHz and is thus wide enough to handle pulses of  $50\mu$  sec width and larger. The over-all gain is 100 db (max). The d.c. level of the quadrature channel outputs is 0 to 10 V and can be adjusted by frontpanel mounted potentiometers. Provision is also available to check for the presence of d.c. off-sets in the quadrature channel outputs and to null them. The input and output impedances are  $50\Omega$ . The receiver requires regulated supply voltages of  $\pm 15V$  (dual) which are fed from commercial units.

### 3.3. Frequency Synthesiser

Solid state hardware (IC chips and transistors) is exclusively used for the frequency synthesiser which is wired on 3 printed circuit cards. The first card accommodates the 10 MHz crystal oscillator, frequency dividers and the logic gates for the generation of the negative and positive Tx pulses. The detailed circuit arrangement is shown in Fig.4. 7437 quadruple 2-input NAND buffer is used as 10 MHz master oscillator with the mounted crystal in its feedback loop

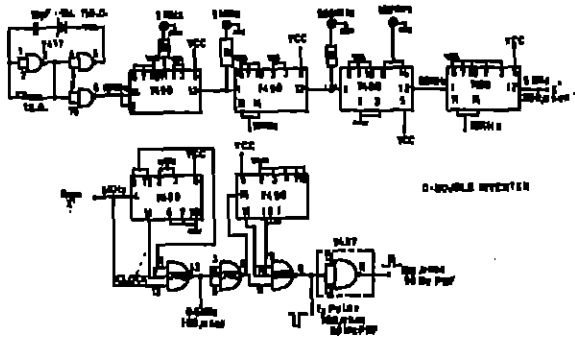


Fig. 4. Circuit diagram of the 10 MHz crystal oscillator, frequency dividers and transmitter rf and keyer pulse generators.

and the output of which is fed to a string of 7490 decade counters. Pulse trains with frequencies of 5.0 MHz and 500 KHz required for synthesising the drive frequency for the Tx and L.O. for the Rx are taken through double inverters (7404) from appropriate points of the divider chain. 7410 triple input NAND gates are used in association with the last two decade scalars of the divider chain to generate the negative and positive pulses to 100  $\mu$  sec width and 50 Hz repetition frequency. The delay gate pulse generator, the circuit of which is given in Fig.5, is wired on the second card. 7485 4-bit magni-

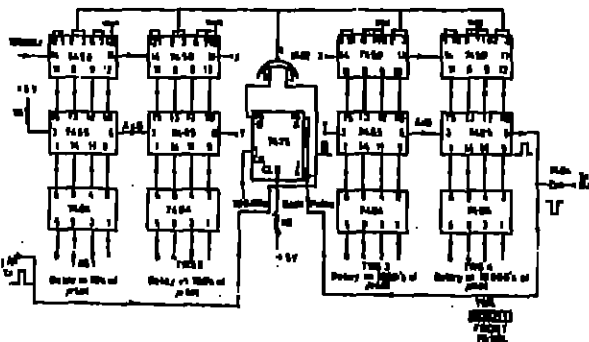


Fig. 5. Circuit diagram of the delay gate pulse generator.

tude comparators, 7490 decade counters, 7476 J-K flip-flops and 7402 2-input NOR gates constitute the hardware used for the

logic designed to generate the gate pulses of 10  $\mu$  sec width. After the counter is initiated by the positive Tx pulse, the comparator output will go high once the two counts match. The high comparator output enables the next pulse to initialise the counter and also increment the counter producing mismatch between the two counts. This renders the comparator output to go low and thus generates pulses of 10  $\mu$  sec width. Four thumb-wheel switches together with 7404 inverters generate the programme of delay for the S/H gate pulse.

The 5.0 MHz and 5.5 MHz (L.O.) signal generators are wired on the third card. The circuit diagrams are shown in Fig.6.

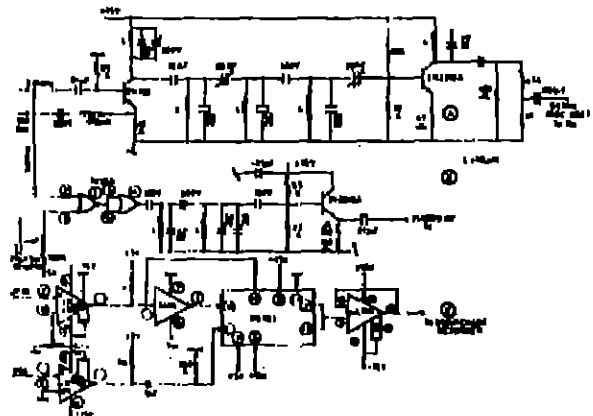


Fig. 6. Circuit diagram of (A) carrier frequency (B) local oscillator frequency generators and (C) logic for recording phase path changes in wavelength ( $\lambda$ ) units.

The 5.0 MHz square waves are filtered in a Butterworth filter to yield a 5.0 MHz CW signal free from higher harmonics, and the output is taken through a current amplifier stage employing 2N 2219A transistor. The 100 $\mu$  sec negative Tx pulse is used to pulse modulate the carrier signal. A 2N 708 transistor is used to mix the 5.0 MHz and 500 KHz square waves and the mixer output is filtered in a 3-section Butterworth filter to remove

all frequency components above and below 5.5 MHz. The filtered output is amplified in a tuned amplifier stage using 2N 2219A transistor and is fed to the receiver through an attenuator.

### 3.4. Logic for Inferring Phase Path Changes

The circuit diagram of the logic scheme adopted to sense and record the changes in phase path in units of  $2\pi$  radians is shown in Fig. 6(C) and is wired on a separate card which is also mounted in the frequency synthesiser unit. The voltage comparators used are LM 311 chips and the analog gate used is the Siliconix DG 181 chip.  $\mu$  A741 linear operational amplifier and 7404 inverter are the other hardware used in the logic scheme. All digital I.C. chips are operated with a regulated supply of +5V and all transistors and linear IC's with  $\pm 15V$  (dual) derived from commercial units.

## 4. Observations and Discussion

The sounder is operated regularly during day light hours for about 4 hrs a day and phase path data are being accumulated under diverse ionospheric conditions. The sounding schedules are restricted to day time in the first instance because the frequency of occurrence of TIDs is quite high during day time than during night. We present in this section a brief account of the general features of the phase path variations of F-region reflections noticed in the first few months of data acquisition. The procedures for recording and data reduction are as follows. The quadrature outputs (before S/H circuits) of the receiver are monitored on a dual beam oscilloscope and the rf attenuation is adjusted so as to give an output of about 3V in both the channels. The channel outputs are also checked for the presence of d.c. off-set.

The delay of the S/H gate pulse is adjusted to select the altitude region of interest and is made to coincide with the ionospheric echo maximum. Monitoring of the channel outputs is continued throughout each data run to observe and record the prevailing ionospheric conditions and to make adjustments of the rf attenuation and gate pulse delay, if required. The data are scaled by simply counting the total number of pulses (each pulse corresponding to a phase path change of  $1\lambda$ ) that occurred during time intervals of 30 sec., taking into account the sign of the pulses. The cumulative sum of the phase path changes in successive 30 sec intervals is then taken as the temporal variation of phase path.

Following the above analysis procedure, it is found that the phase path variation of F-region reflections on 5.0 MHz (true height of reflection around 190 km) at Kodaikanal consistently shows a general decrease in the forenoon period and a general increase in the afternoon period, as may be seen from the typical examples presented in Fig.7. The magnitude of the steady decrease (increase) in the forenoon (afternoon) hours is noticed to undergo considerable changes from day-to-day. The steady components in the temporal variation of phase path can be attributed, on theoretical grounds, to the diurnal changes in the true height of reflection and/or changes in the electron density profile below the reflection level with the solar zenith angle. It is also to be noted that besides production and loss of ionization due to photoionization and recombination processes, there are other mechanisms such as vertical drifts which can affect the electron density at all levels in the ionosphere. The vertical drift is particularly important at low dip latitudes. Ray tracing and modelling studies based on



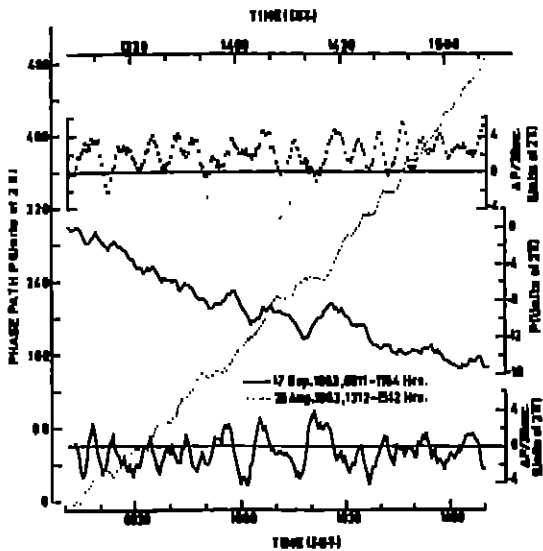


Fig. 7. Variation of phase path (P) with time of reflection from F-region over Kodaikanal during prenoon and postnoon hours. Also shown are the plots of the 5-point running means of phase path change ( $\Delta P$ ) per 30 sec versus time.

local electron density profiles are needed to assess the relative contributions of the various mechanisms to the steady components and their day-to-day variability. As we have the C-3 ionosonde and La cour magnetogram facilities at Kodaikanal, this work will be attempted as soon as adequate data is acquired. It is also noticed that superposed on the steadily decreasing (increasing) phase path in the forenoon (afternoon) hours, small scale oscillations in phase path invariably manifest as may be seen from the typical data presented in Fig.7. To bring out these small scale perturbations more clearly, the phase path (P) versus time curve is differentiated and 5-point running averages of the phase path change ( $\Delta P$ ) per unit time (30 sec) are evaluated and plotted. The running mean values of  $\Delta P$  are also subjected to spectral analysis using the maximum entropy method (MEM) to infer the spectral content of the small scale fluctuations. The length of the prediction error filter (PEF) is taken

as 25 percent of the sample length in computing the frequency spectrum of  $\Delta P$  adopting the algorithm of Radoski et al. (1975). The results of these operations with the data recorded so far demonstrated that wavelike distortions in phase path with peak-to-peak amplitudes of  $5-10 \lambda$  (300-600 metres) and periods in the range 5-20 min occur with reflections from lower thermosphere in the vicinity of the dip equator. This feature may be seen from Figs 7 and 8 when in the

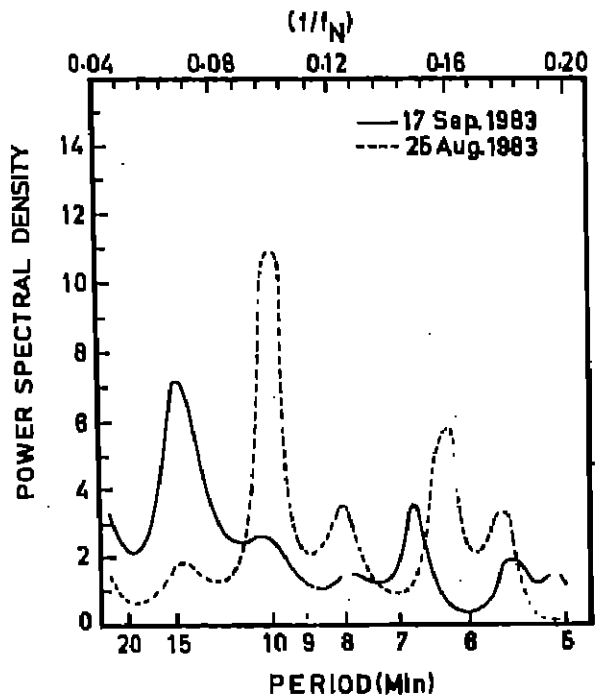


Fig. 8. Power spectra of  $\Delta P$  corresponding to records of Fig.7.

plots and frequency spectra of  $\Delta P$  corresponding to the typical data of fig.7 are presented. The frequency spectra of  $\Delta P$  also exhibit an interesting property namely, an increase in the amplitude of the perturbations with their period. The peak-to-peak amplitude and dominant periods of the fluctuations are, however, found to vary from one day to another. These results, although preliminary, are the first ones of their kind obtained

in the Indian electrojet region. The observed small scale quasi-periodic fluctuations in phase path are attributed to atmospheric gravity waves since their dominant wave periods fall well within the expected frequency spectrum of gravity waves at F-region altitudes and they exhibit one of the characteristics of gravity waves namely, the increase of amplitude with increase in period of the wave.

Besides as a tool for the detection and study of TIDs, the phase path sounder can profitably be used for other ionospheric investigations because of the excellent temporal resolution it offers, and its inherent capability to measure even extremely small variations in phase path. For example, the rapid changes in the ionosphere that occur in association with geophysical events like solar flares, solar eclipses, geomagnetic sudden commencements and geomagnetic micropulsations can be studied. The scope of investigations can also be widened by augmenting the basic system described here with additional facilities. Some feasible configurations which will be taken up for development shortly are outlined in the following. Recording of phase path variations with a single receiving antenna gives only a limited information on TIDs (wave period and amplitude). The phase path sounder, if operated with a set of three receiving antennae situated at the corners of a right angled isosceles triangle, will yield additional information such as the speed and direction of propagation of TIDs, and will help to gain an insight into the possible source(s) of TIDs. Simultaneous recording of the phase path variations of reflections from different altitude regions, which can be done by duplicating some of the existing circuitry, during phenomena like blanketing sporadic-E( $E_{sb}$ ) and equatorial spread-F (ESF) can lead to a better under-

standing of the dynamics and structure of the ionosphere. The experimental set-up can also be developed as a phased array synthetic aperture system of spaced antennas to measure the direction of arrival of ionospheric reflections with an accuracy better than  $1^\circ$  (Balan et al. 1979). It is to be emphasised in this context that as the basic system is augmented and operated with multiaerial and/or multiheight facilities, the number of strip chart data channels will increase manifold leading to data handling and analysis problems. To cope up with these, a digital tape recording facility needs to be developed.

Digital recording also helps to realise the intrinsic capability of the system to measure phase path changes with an accuracy of about  $15^\circ$ . The quadrature channel arrangement of the phase coherent receiver used renders the present system readily adoptable for digital tape recording and computer processing.

#### Acknowledgements

The work forms a part of the development programme of the Solar-Terrestrial Relationships group of the institute. The authors are grateful to (Late) Professor M.K.V.Bappu and Professor J.C.Bhattacharyya for their keen interest and encouragement. One of the authors (J.H.S) is grateful to DR. C.R.Reddi, Space Physics Division, VSSC, Trivandrum, for many useful discussions and suggestions concerning the experimental set-up.

#### References

- Balan, N., Nandakumar, V.N., Chandrasekhar, S., Iyer, K.N., Rao, P.B., and Sridhar, A., 1979, Indian J. Rad. Space Phys. **0**, 289.
- Butcher, E.C., Joyner, K.H., 1972, Planet. Space Sci. **20**, 613.

- Francis, S.H., 1975, *J. Atmos. Terr. Phys.* **37**, 1011.
- Genova, F., Aubler, M.G., 1983, *Ann. Geophys.* **1**, 415.
- Meyer-Vernet, N., 1980, *Astr. Astrophys.* **84**, 142.
- Meyer-Vernet, N., Daigne, G., Lecacheux, A. 1981, *Astr. Astrophys.* **96**, 296.
- Nagpal, O.P., 1977, *Indian J. Rad. Space Phys.* **6**, 180.
- Radoski, H.R., Fougere, P.F., Zaalick, E.J., 1975, *J. Geophys. Res.* **80**, 619.
- Reddi, C.R., 1969, Ph.D thesis, Andhra Univ.
- Reddi, C.R., Murthy, B.V.K., Subba Rao, K.S.V., Khosla, K.P., Rao, P.B., Balan, N., 1980, VSSC Tech. Rep. No.46.
- Reddi, C.R., Rao, B.R., 1967, *Radio. Electronic. Engrs.* **34**, 53.
- Reddi, C.R., Rao, B.R., 1971, *J. Atmos. Terr. Phys.* **33**, 251.
- Rottger, J., 1977, *J. Atmos. Terr. Phys.* **39**, 987.
- Sastri, J.H., Murthy, B.S., 1977, *J. Geomag. Geoelectr.* **29**, 497.
- Schrader, D.H., Fraser, A.D., 1975, *J. Atmos. Terr. Phys.* **37**, 429.
- Somayajulu, V.V., Reddy, C.A., Viswanathan, K.S., 1980, *Cospar Symposium Series 8*, Pergamon Press, p.25.
- Srivastava, S.K., Pradhan, S.M., Singh, B., Tantry, B.A.P., 1971a, *Indian J. Pure. Appl. Phys.* **9**, 609.
- Srivastava, S.K., Pradhan, S.M., Tantry, B.A.P., 1971b, *Ann. Geophys.* **26**, 881.